VIRTUAL WORKSHOP ON OPTICAL SENSORS FOR ENERGY APPLICATIONS

Argonne NATIONAL LABORATORY

# INFRARED AND MICROWAVE SENSORS AND SYSTEMS FOR NUCLEAR ENERGY APPLICATIONS

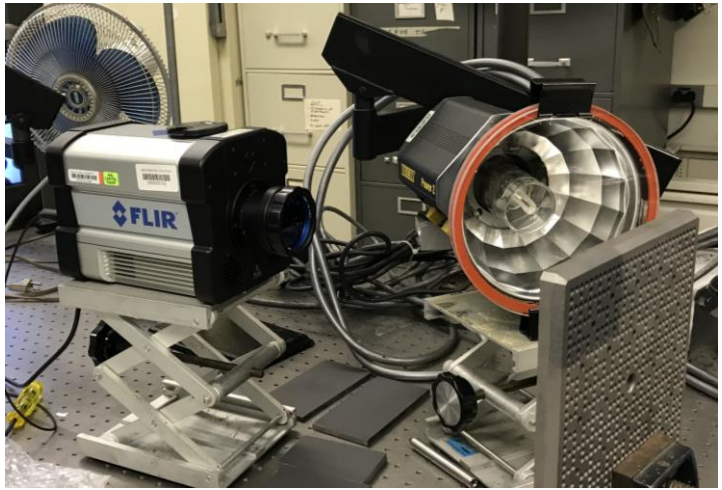


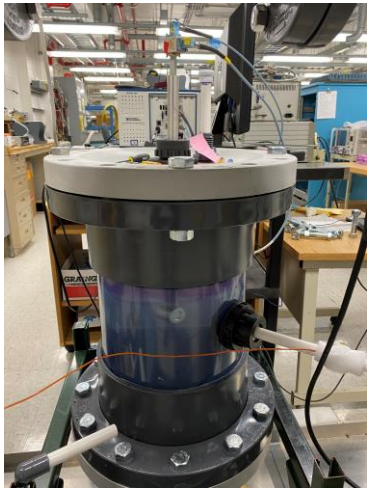

**ALEXANDER HEIFETZ**

Argonne National Laboratory

University of Pittsburgh

March 2, 2023

# OUTLINE

- Infrared (λ ~ 3-5μm) thermography for nondestructive evaluation of additively manufactured metals
  - System design & machine learning/signal processing
  - Sponsor: NEET AMM

- Microwave (λ ~ 1.5cm) resonant cavity transducer of flow sensing in advanced reactor temperature fluids
  - FOAK sensor design and demonstration
  - Sponsor: NEET ASI

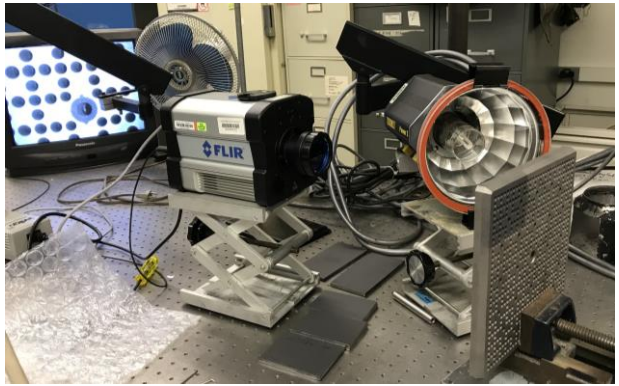


# TEAM ACKNOWLEDGEMENT


- Argonne
  - Xin Zhang (ANL & IIT), Tianyang Fang (ANL &IIT), Thomas Elmer, Dick Koehl, Darius Lisowski, HT Chien, Sasan Bakhtari
- Collaborators
  - Jafar Saniie (IIT)
  - Anthonie Cilliers (Kairos Power)
  - Bill Cleary (Westinghouse)
  - Boris Khaykovich (MIT Nuclear Reactor Laboratory)
  - Miltos Alamaniotis (UTSA)
- SULI Students
  - Tori Ankel (UChicago), Dmitry Shribak (UChicago), Zoe Fisher (MIT), Elaine Jutamulia (MIT), Tiffany Liu (Berkeley), David Aronson (UIUC), Gabby Carrel (UCSB)

# PULSED INFRARED THERMOGRAPHY FOR NONDESTRUCTIVE EVALUATION OF ADDITIVELY MANUFACTURED METALS

# ADDITIVE MANUFACTURING FOR NUCLEAR ENERGY

- Advantages of AM
  - Fabrication of complex shape structures from high-strength and difficult-to-machine metals
    - SS316, IN718, refractory metals
- AM process for nuclear applications
  - Laser powder bed fusion (LPBF)
    - Selective laser melting (SLM) of microscopic metallic grains with $T_{melt} \sim 1400^{o}C$

Metallic Powder

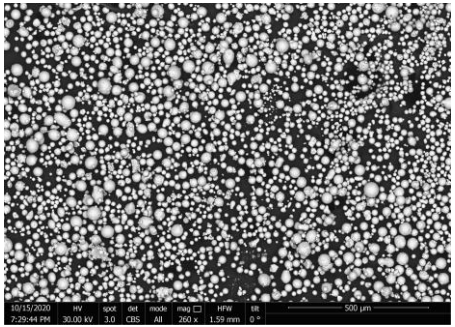

<D> = 50µ

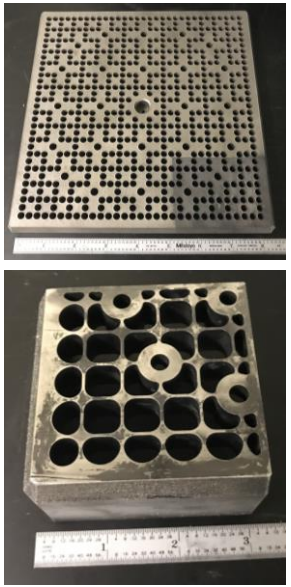

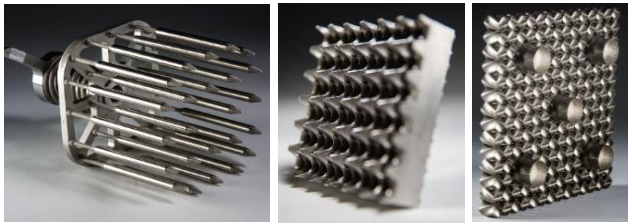

Westinghouse AM structures

A. Heifetz, et. al. *Trans. Am. Nucl. Soc*. 121, 589-591 (2019).

# METAL DEFECTS IN LASER POWDER BED FUSION MANUFACTURING

- Pores may cause crack initiation
  - Probability is higher for larger (>20μm) and closer to surface pores

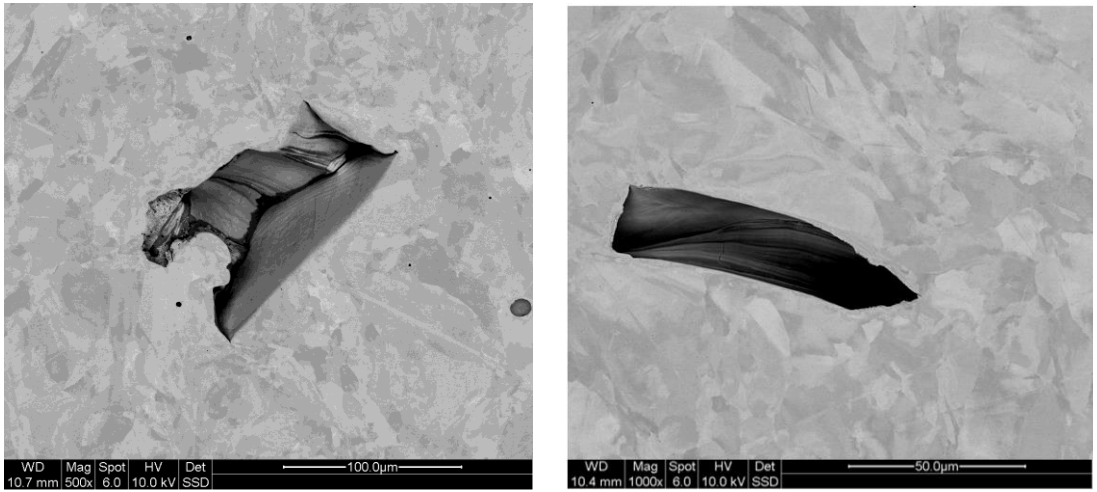


ANL images (IVEM-NSE)

SEM images of pores in SS316 printed with LPBF

- Need quality control of actual 3D printed structures

# QUALITY CONTROL OF ACTUAL STRUCTURES

- Nondestructive imaging of sub-surface pores with pulsed infrared thermography
  - Apply pulse of thermal energy to material surface with flash lamp
  - Record surface temperature transients T(x,y,t) with IR camera

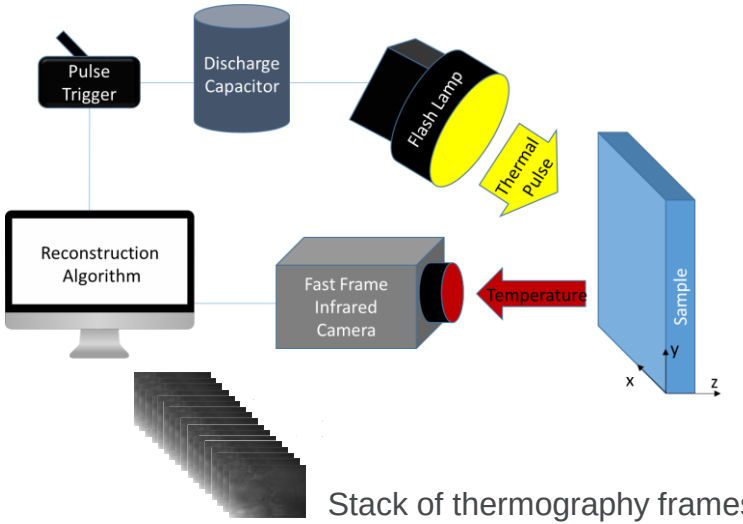


Stack of thermography frames

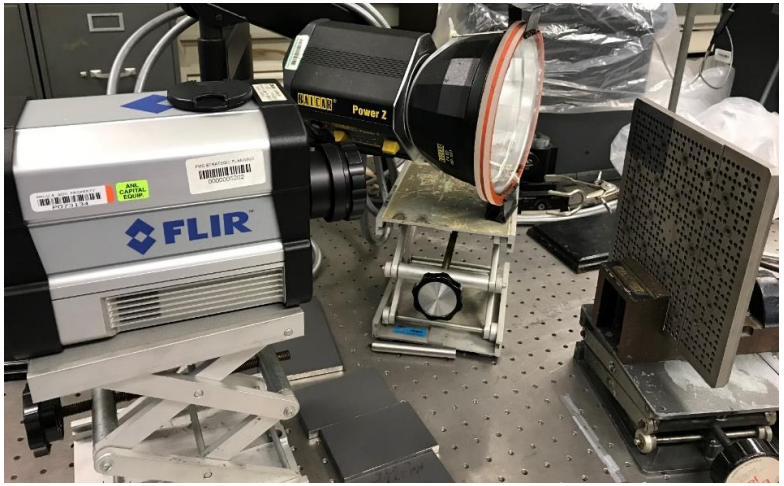


FLIR x8501sc MWIR 1280x1024 at 180fps

X. Zhang, J. Saniie, W. Cleary, A. Heifetz, “Quality Control of Additively Manufactured Metallic Structures with Machine Learning of Thermography Images,” JOM 72(12),4682-4694 (2020)

# PRINCIPLE OF INTERNAL DEFECT DETECTION

- Temperature “hot spots” can be observed on the material surface above the flaw
- Demonstrated with COMSOL computer simulations
  - Time evolution of heat transfer through metallic plate
  - Appearance of localized “hot spot” on the plate front surface

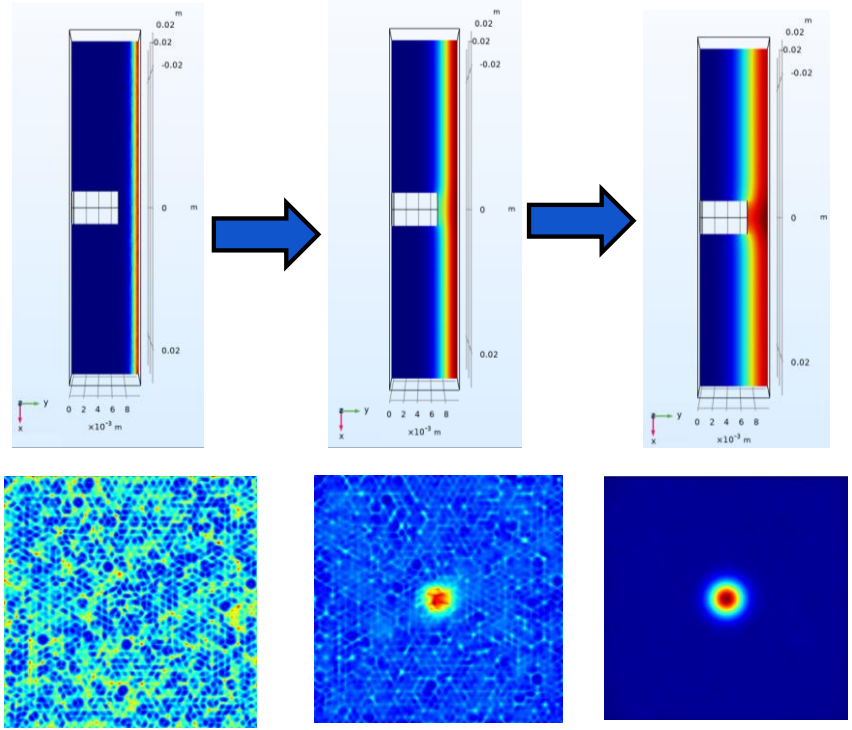

X. Zhang, J. Saniie, A. Heifetz, “Detection of Defects in Additively Manufactured Stainless Steel 316L with Compact Infrared Camera and Machine Learning Algorithms,” JOM, 72(12), 4244-4253 (2020)

# ADVANTAGES OF THERMOGRAPHY

| | X-Ray/Neutron CT | Ultrasonic | Thermography |
|---|---|---|---|
| Non-contact | Yes | No | Yes |
| Compact | No | Yes | Yes |
| 2-D Imaging | Yes | No | Yes |
| One-sided | No | Yes | Yes |

# ENHANCING THERMOGRAPHY IMAGES WITH MACHINE LEARNING ALGORITHMS

## Neural learning blind source separation

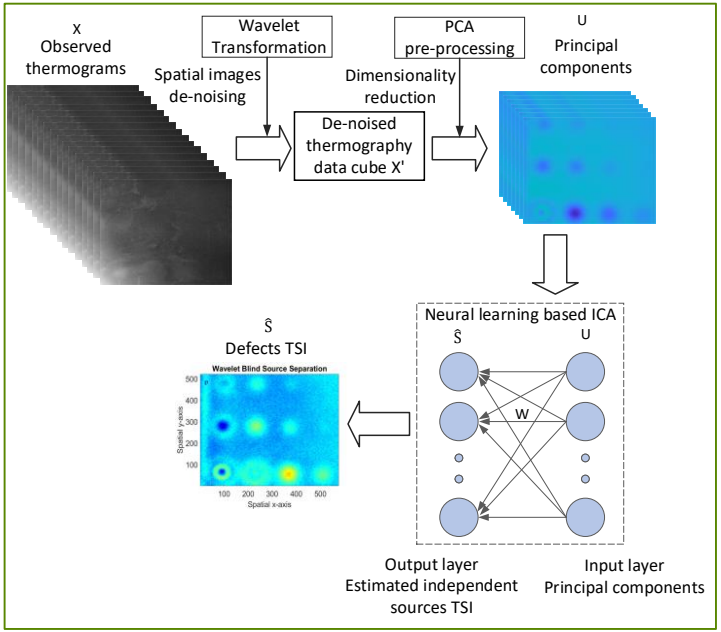


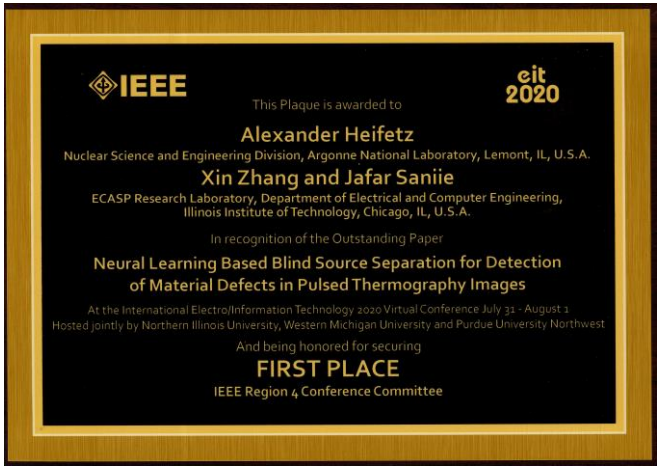


X. Zhang, J. Saniie, A. Heifetz, “Neural Learning Based Blind Source Separation for Detection of Material Defects in Pulsed Thermography Images,” *IEEE International Conference on Electro Information Technology* (EIT2020), 112-116

# STRATEGY FOR DEFECTS DETECTION STUDIES

- Develop metallic specimens with calibrated defects
  - Specified size and depth
- Two types of defect models
  - Flat bottom hole indentations
  - Defects imprinted during additive manufacturing containing trapped un-sintered powder

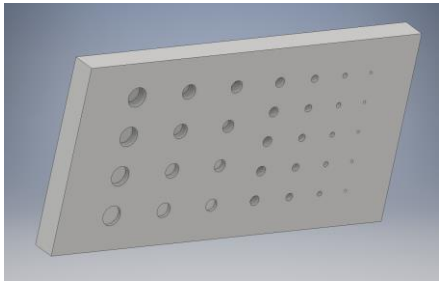

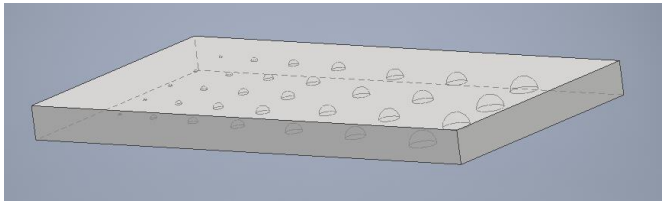

# INVESTIGATING DEFECT IMAGING LIMITS

## LPBF-Imprinted Defects 1mm to 250µm

- LPFB-imprinted hemisphere with un-sintered powder SS316 plate at Westinghouse

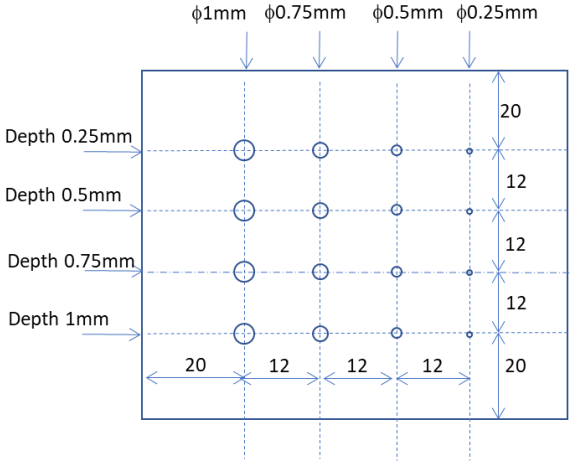


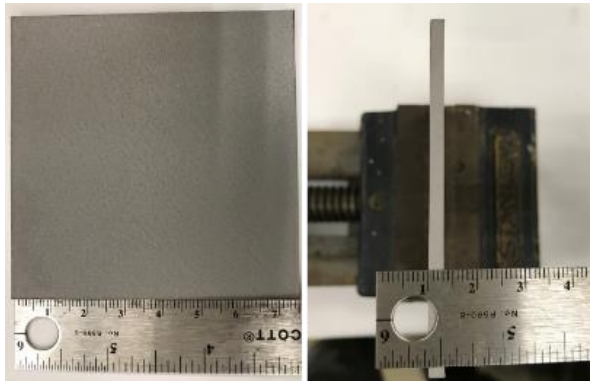

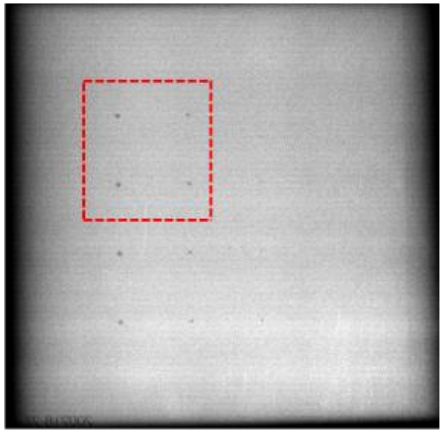

75keV transmission X-ray 30µm/pixel

# INVESTIGATING DEFECT IMAGING LIMITS

## LPBF-Imprinted Defects 1mm to 250µm

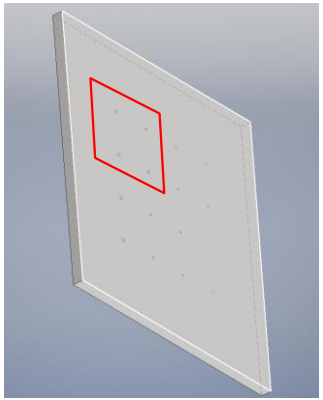

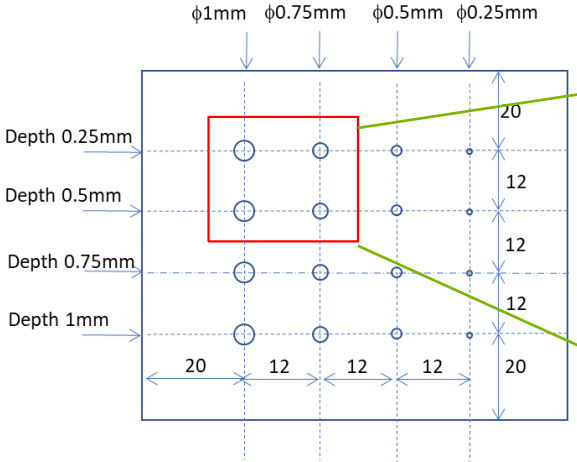


Processed Image

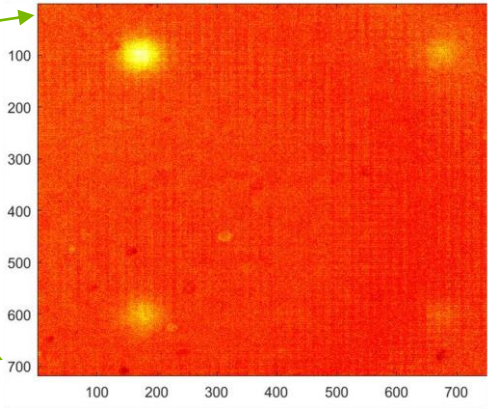


FLIR x8501 set to 768x768 pixels array, 268fps

- Smallest detected defect thus far 750µm

X. Zhang, J. Saniie, S. Bakhtiari, A. Heifetz, “Compression of Pulsed Infrared Thermography Data with Unsupervised Learning for Nondestructive Evaluation of Additively Manufactured Metals,” *IEEE Access* 10, 9094 – 9107 (2022).

# INVESTIGATING DEFECT IMAGING LIMITS

## Flat bottom hole indentation defects imaged from flat side

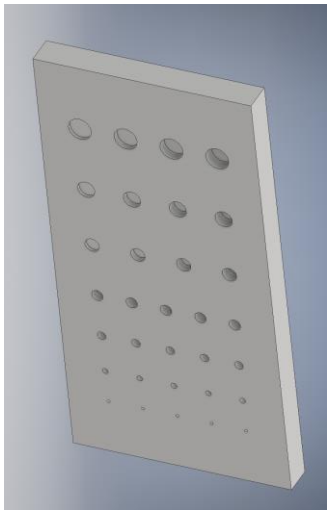

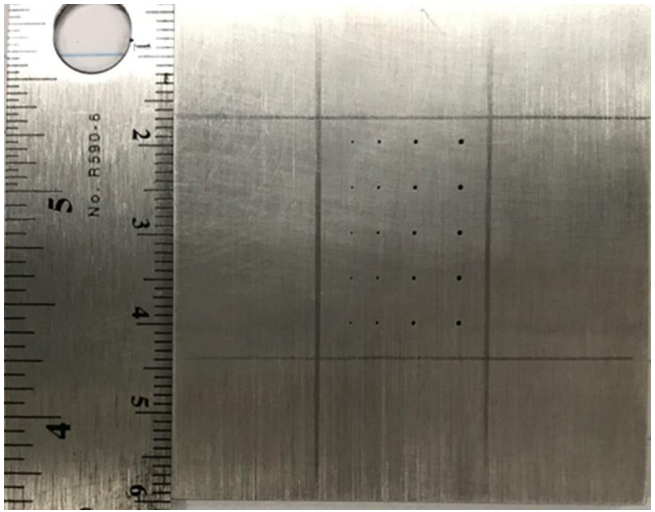

EDM-drilled microscopic FBH's in SS316 plate

Back surface painted with Krylon ultra flat black spray paint

# INVESTIGATING DEFECT IMAGING LIMITS

## Flat Bottom Hole Defects

3mm-thick plate

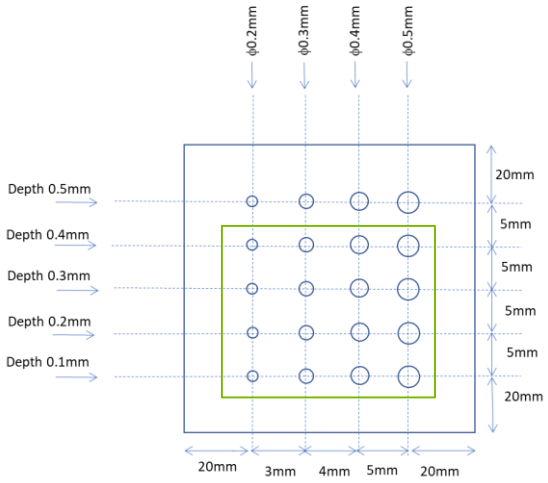


Recording

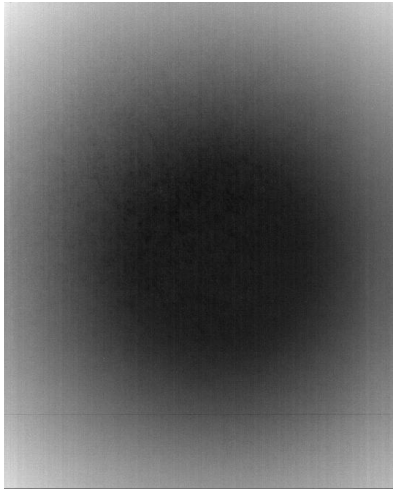

Processed

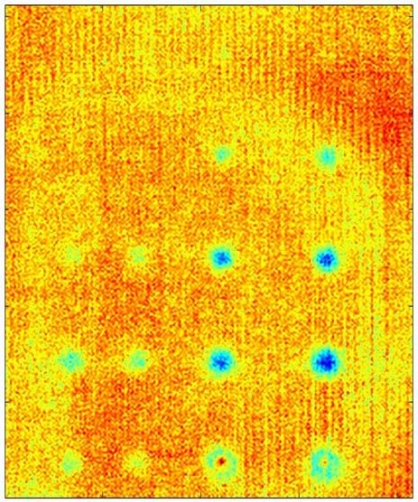

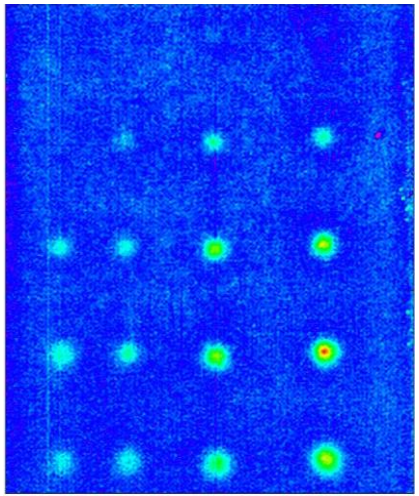

SS316

IN718

Smallest detected defect 200µm

1024x800 pixels, 180Hz frame rate

# INVESTIGATING DEFECT IMAGING LIMITS

## FBH Microscopic Defects 203µm to 127µm in SS316

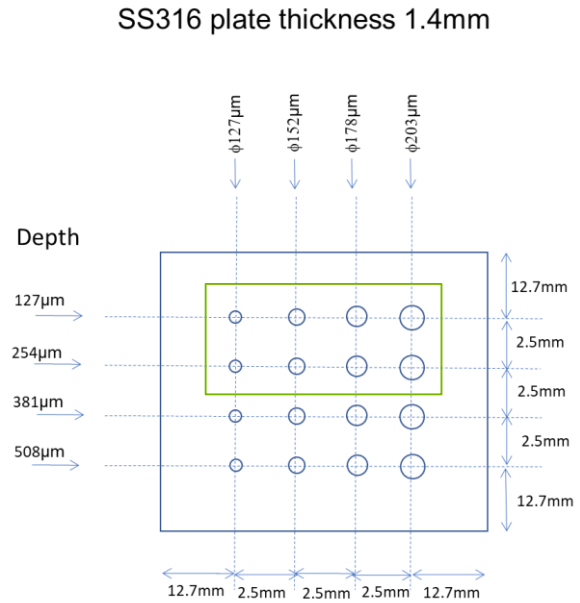


Recording

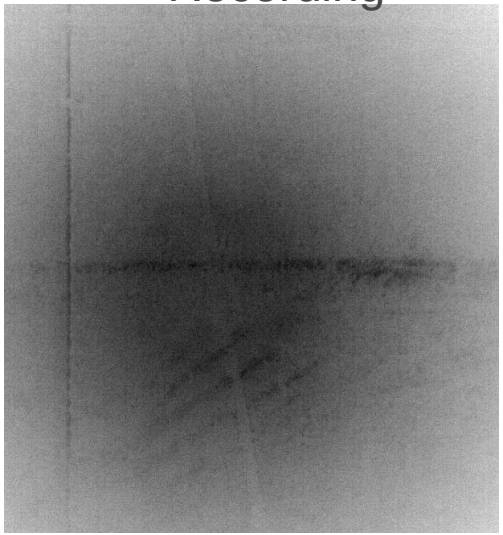

Processed

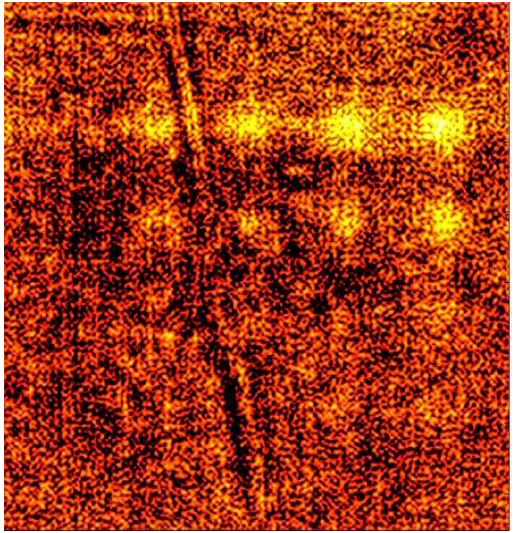

Smallest detected defect 127µm

Frame Rate: 220 Hz; window size: 752 x 704

# INVESTIGATING DEFECT IMAGING LIMITS

## FBH Microscopic Defects 152µm to 76µm in SS316

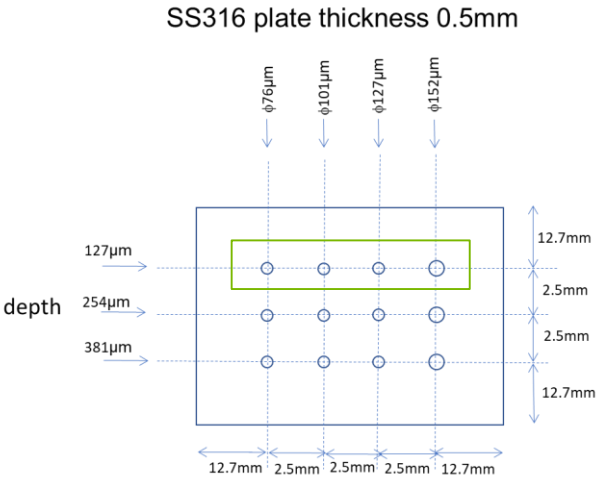


Recording

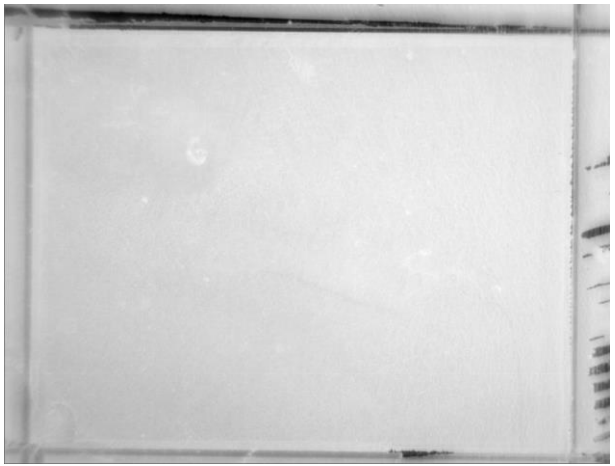

Processed

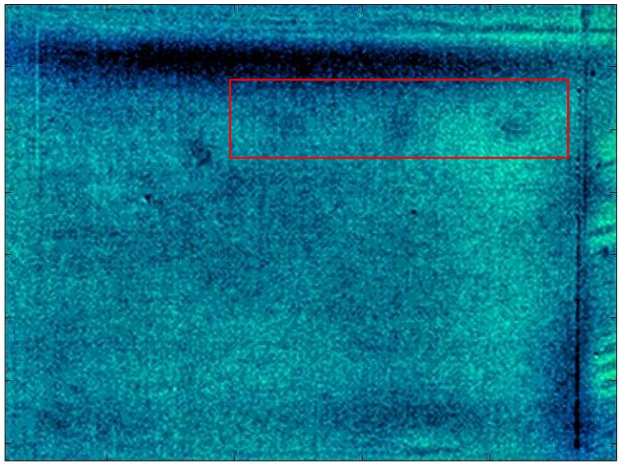

Smallest detected defect 101µm

Frame Rate: 240 Hz; window size: 728 x 960

# DEPTH RECONSTRUCTION FROM THERMOGRAPHY DATA CUBE

- Reconstruction based on 1-D model of heat transfer

$$\frac{\partial T}{\partial t} = \alpha \frac{\partial^2 T}{\partial z^2} \qquad \alpha = k/\rho c$$

  - α is thermal diffusivity defined as
  - ρ is the density, c is the specific heat, k is the thermal conductivity

- Effusivity is a measure how material exchanges thermal energy with its surroundings $e = (\rho c k)^{1/2}$

- Characteristic relationship between depth and time is $z = (\pi \alpha t)^{1/2}$

- From analytic solution for semi-infitine medium
  - Q is the instantaneously deposited surface thermal energy density

$$e(t) = \frac{Q}{T(z=0,t)\sqrt{\pi t}}$$

- Reconstruction of spatial effusivity

$$e(z) = z \frac{2Q}{\pi\sqrt{\alpha}} \frac{d}{dt}\left(\frac{1}{T(t)}\right)\Big|_{t=z^2/\pi\alpha}$$

Example: effusivity reconstruction for a 5mm-thick plate

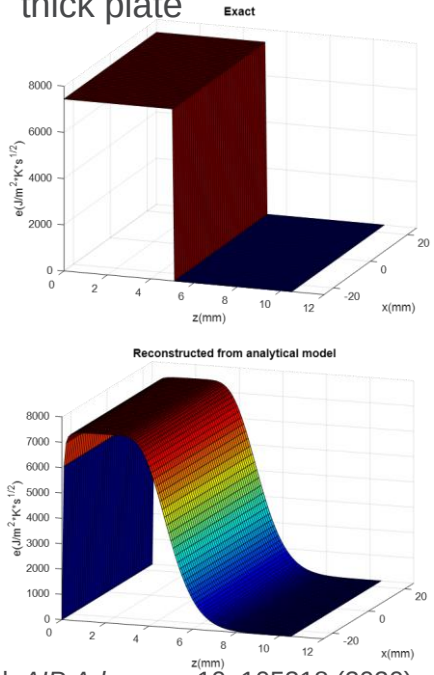


A. Heifetz, et. al. *AIP Advances* 10, 105318 (2020)

# THERMAL TOMOGRAPHY (TT) IMAGING OF IN718 PLATE

XY plane

Parallel plane cross-section reconstructions

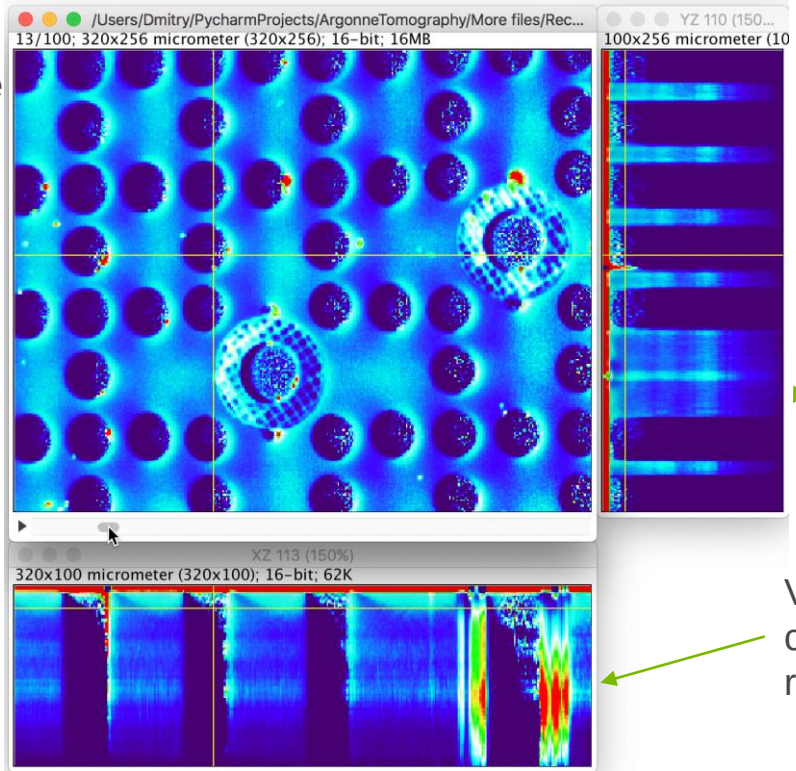


YZ plane

XZ plane

Vertical plane cross-section reconstructions

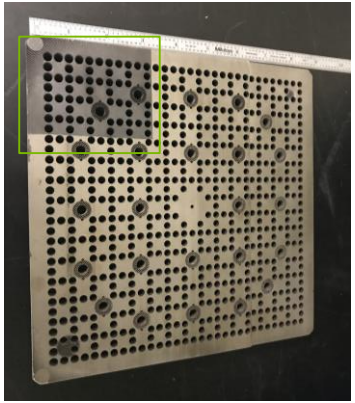

Imaging time 20s to scan 3in x 2in x 2/3in section of 8in x 8in x 2/3in plate

# TT IMAGING OF FBH CALIBRATED DEFECTS

- Flat bottom holes in SS316

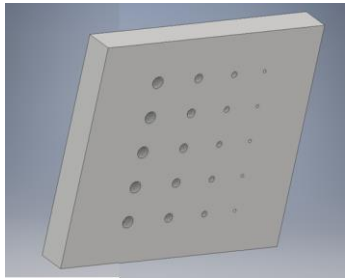


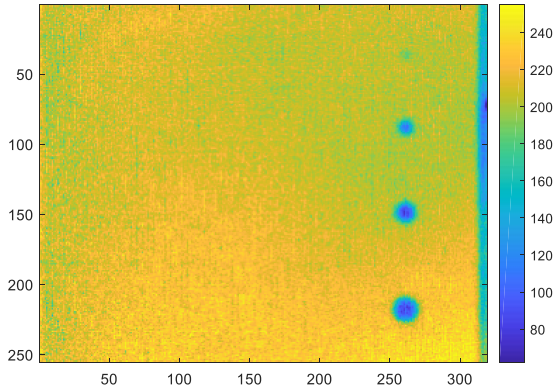


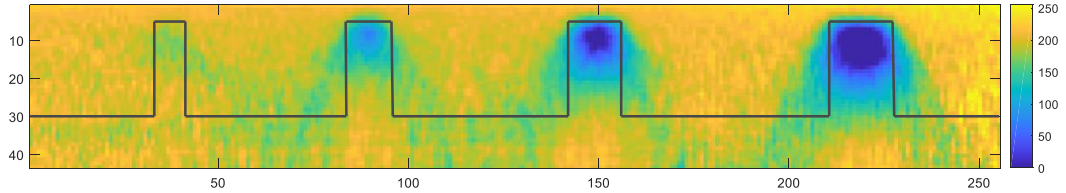


A. Heifetz, D. Shribak, X. Zhang, J. Saniie, Z.L. Fisher, T. Liu, J.G. Sun, T. Elmer, S. Bakhtiari, W. Cleary, “Thermal Tomography 3D Imaging of Additively Manufactured Metallic Structures,” AIP Advances 10(10), 105318 (2020).

# TT IMAGING OF LPBF-IMPRINTED CALIBRATED DEFECTS

- Imprinted hemispherical regions containing un-sintered powder in IN718

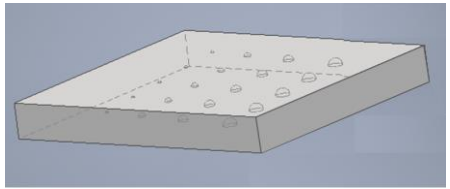

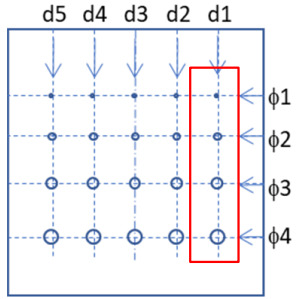


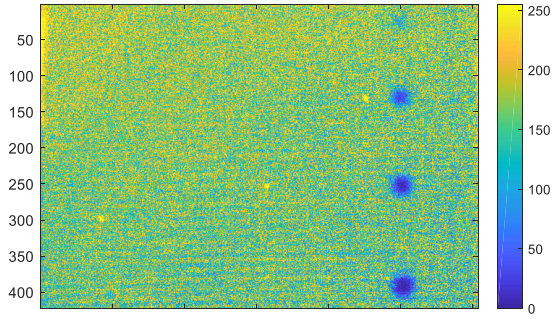


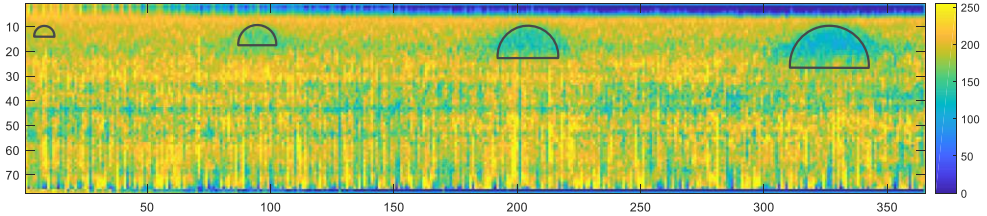


A. Heifetz, et. al. *AIP Advances* 10, 105318 (2020)

# AUTOMATED CLASSIFICATION OF DEFECTS IN TT IMAGING

- Classification of defects with convolutional neural network (CNN) trained on elliptical defects

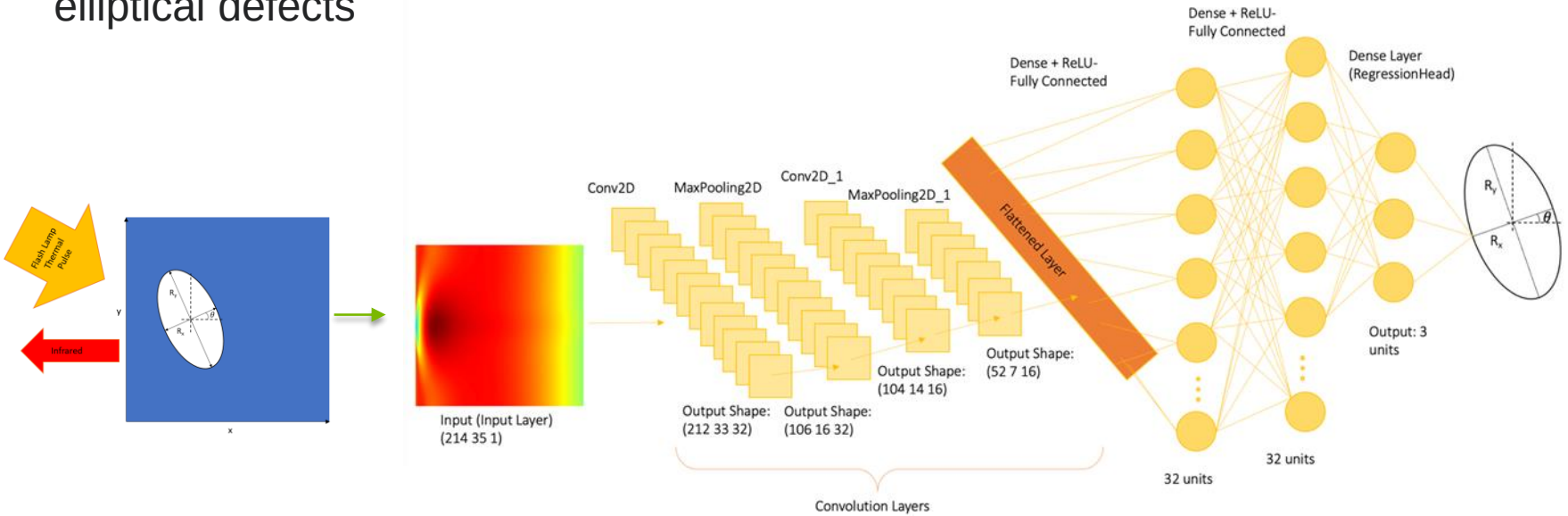


Computer-simulated thermal tomography

V. Ankel, D. Shribak, W.-Y. Chen, A. Heifetz, “Classification of computed thermal tomography images with deep learning convolutional neural network,” Journal of Applied Physics 131, 244901 (2022) (Editor’s Pick)

# CLASSIFICATION OF DEFECTS

Source image

Computer-generated TT reconstructions of plates with rotated defects

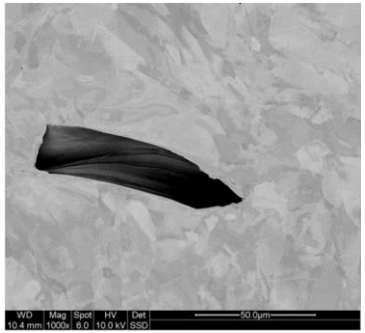


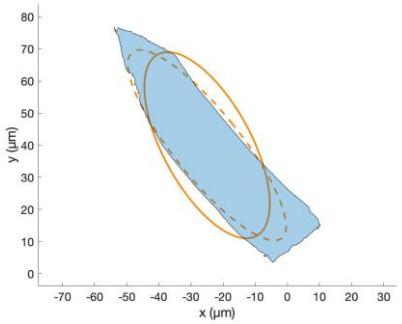


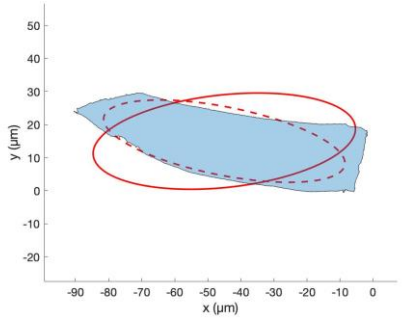


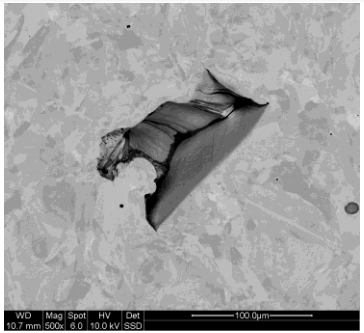


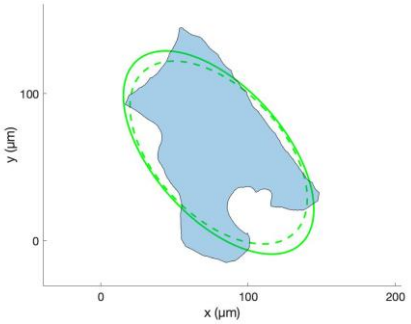


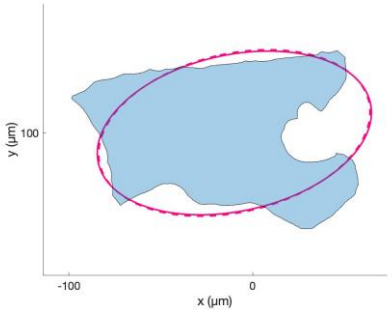

# MICROWAVE RESONANT TRANSDUCER FOR FLOW SENSING IN ADVANCED REACTOR HIGH TEMPERATURE FLUIDS

# OVERVIEW

Develop multimodal immersion sensor of high temperature fluid

- Hollow metallic cylindrical microwave resonator with thin flexible membrane
  - Resilient to high temperature and radiation
  - Communication with sensor through hollow rigid metallic microwave waveguide
- Transduction through microscopic volume change that shifts resonant microwave frequency
  - Membrane deflection through dynamic fluid pressure – flow
  - Membrane deflection through static fluid pressure – level
  - Thermal expansion of cylinder – temperature

Applicable to sensing coolant fluid in sodium fast reactor (SFR) and molten salt cooled reactor (MSR)

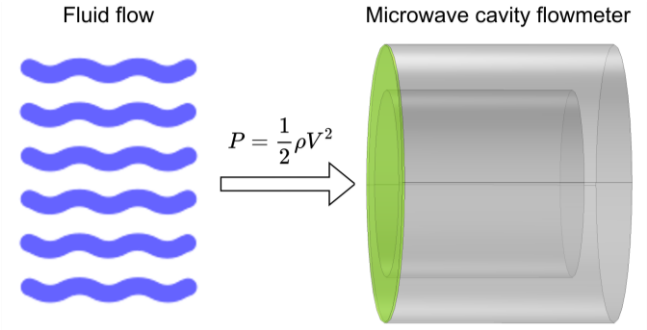

# COMPARISON TO STATE-OF-THE-ART

| | Ultrasonic | Electromagnetic | Anemometry | Microwave Resonant Cavity-Based |
|---|---|---|---|---|
| **Sensing in which fluid** | Liquid sodium & molten salt<br>Based on detection of time of flight or Doppler frequency shift | Liquid sodium<br>Take advantage of electrical conductivity of liquid sodium | Liquid sodium & molten salt<br>Based on convective heat transfer by moving fluid | Liquid sodium & molten salt<br>Transduction is based on fluid-structure interaction |
| **Immersion or external** | External<br>Two transducers in pitch-and-catch or transmission mode require direct line of sight | Immersion or external<br>Measure rate of conducting flux passing through coil cross-section | Immersion<br>Involves measuring reference source cooling rate due to convective heat transfer | Immersion<br>Can be made as small as type-K thermocouple |
| **Deployment challenges** | Crystal can degrade due to exposure to high temperature and radiation | Permanent magnet could be de-magnetized. Coil requires large size DC power supply | Relatively slow because of heat transfer | Hollow stainless steel structure resilient to high temperature and radiation |

# SENSOR MODEL

Developed analytic sensor model

- Chose right circular cylinder design (L=2a) to achieve highest Q-factor
- Focused on low order $TE_{011}$ mode

$$\Delta f_{nml}^{TE} = \frac{c}{2\pi L\sqrt{\mu_r \varepsilon_r}}\sqrt{\left(2X'_{nm}\right)^2 + \left(l\pi\right)^2}\left(\frac{\Delta L}{L}\frac{\left(l\pi\right)^2}{\left(2X'_{nm}\right)^2 + \left(l\pi\right)^2}\right)$$

$$\Delta L = \frac{3\left(1-\nu^2\right)}{32E}\frac{a^4}{h^3}\rho \mathrm{v}^2$$

*n,m,l* = mode numbers
*c* = speed of light
$X'_{nm}$ = $n^{th}$ root of the derivative of the $m^{th}$ order Bessel function
*L* = length
*a* = radius
*h* = membrane thickness
$\varepsilon_r$ = relative dielectric permittivity
$\mu_r$ = relative magnetic permeability
E = Young's modulus
$\nu$ = Poisson ratio
$\rho$ = fluid density
v = fluid velocity

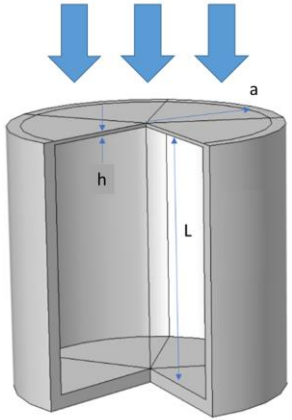


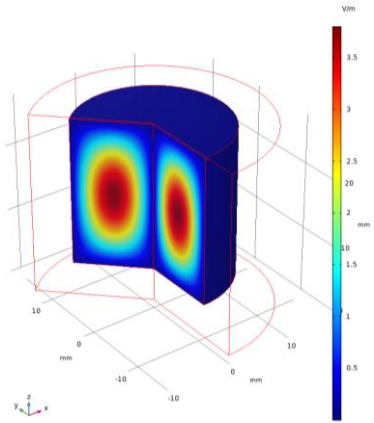

$TE_{011}$ mode

A. Heifetz, V. Ankel, D. Shribak, S. Bakhtiari, A. Cilliers, "Microwave Resonant Cavity-Based Flow Sensor for Advanced Reactor High Temperature Fluids, Proceedings 12th Nuclear Plant Instrumentation, Control and Human-Machine Interface Technologies (NPIC&HMIT 2021), 232–238 (2021).

# SENSOR RESILIENCE ESTIMATION

Conducted preliminary investigation of sensor drift due to membrane creep at high temperature

- Model implemented in COMSOL Structural Mechanics Module
- Combines Nabarro-Herring and Coble creep models
  - Arrhenius's Law type
  - Diffusion driven, high temperature, low stress
- Predict significant creep (>20% of displacement) after $10^4$ hours (417 days) at constant T > 600C and 3kPa load
- Can be compensated during real-time flow measurements by monitoring temperature history

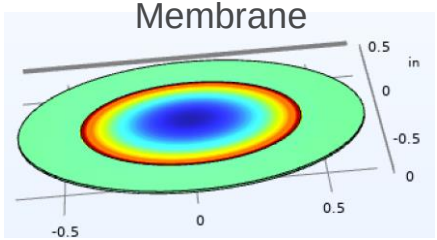


0.008in thickness

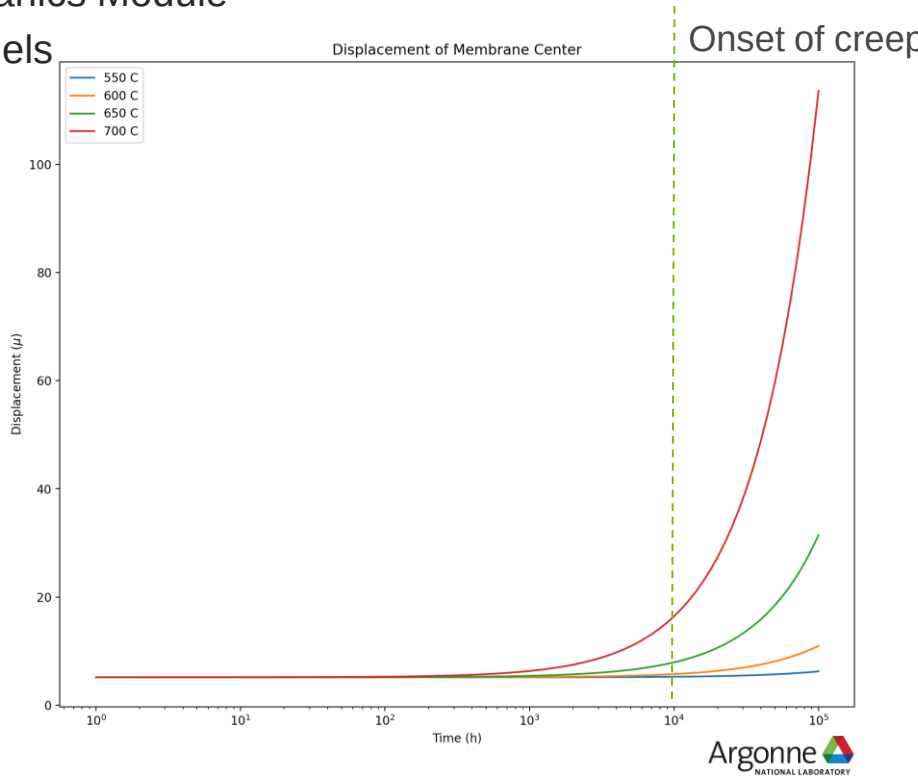

# DEVELOPMENT SCHEDULE

## Sensor prototype design

## Flow sensing in water

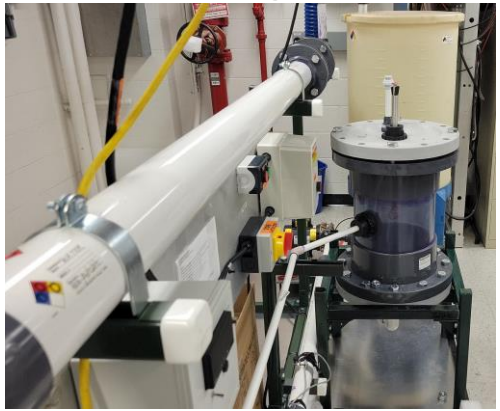

## Flow sensing in high temperature fluid

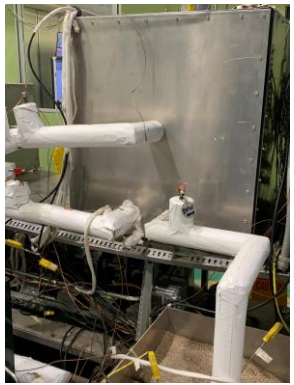


## Current Status

# SENSOR DESIGN

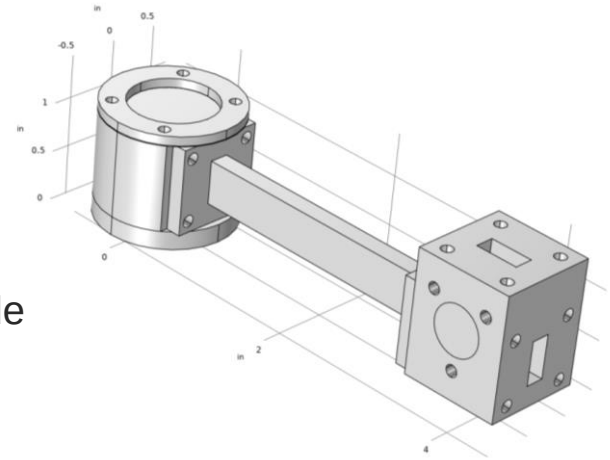

Designed K-band (18-26.5GHZ) microwave cavity

- Cavity excited through subwavelength hole
- Signal readout with a microwave circulator
- Dimensions matched to commercial WR-42 microwave waveguide 22.2mm flange
- Membrane thickness 8mil = 203µm
- Fabricated Brass cavity prototype for initial testing in water

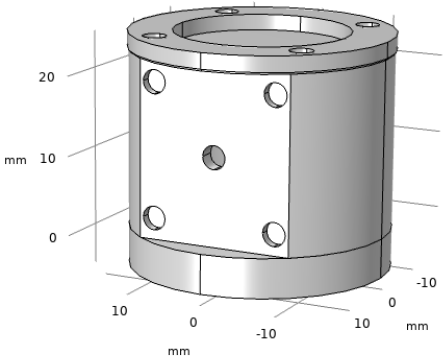


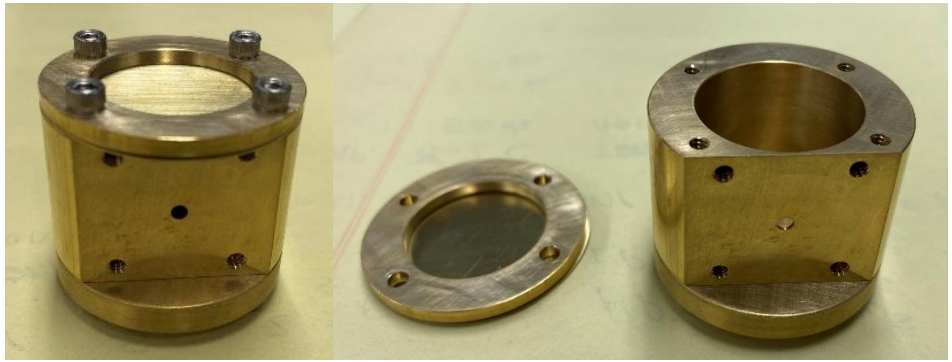

# FLOW SENSING IN WATER LOOP

Developed water flow loop for proof-of-principle tests

- Pump rated up to 60gpm flow rare at ambient pressure
- Omega flowmeter installed for reference flow measurements

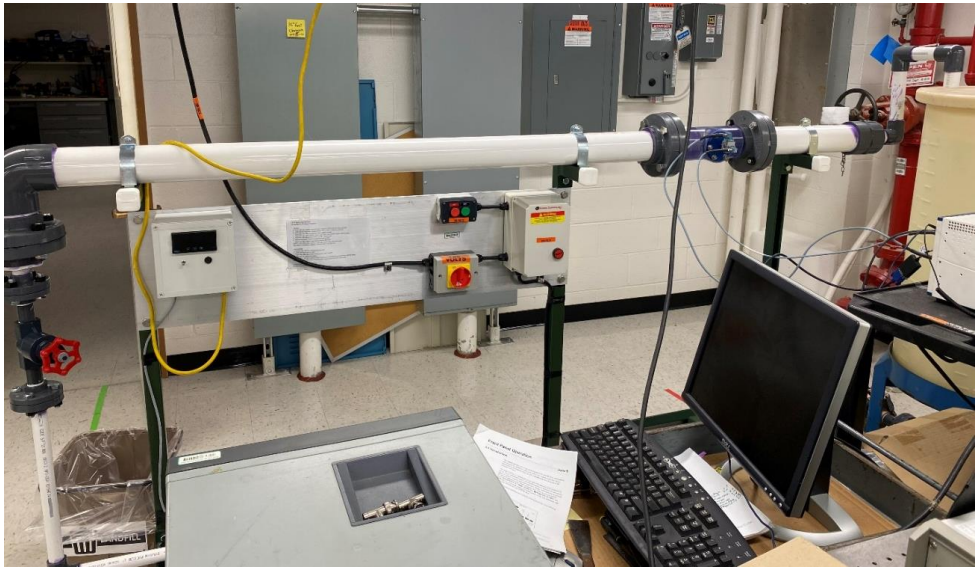

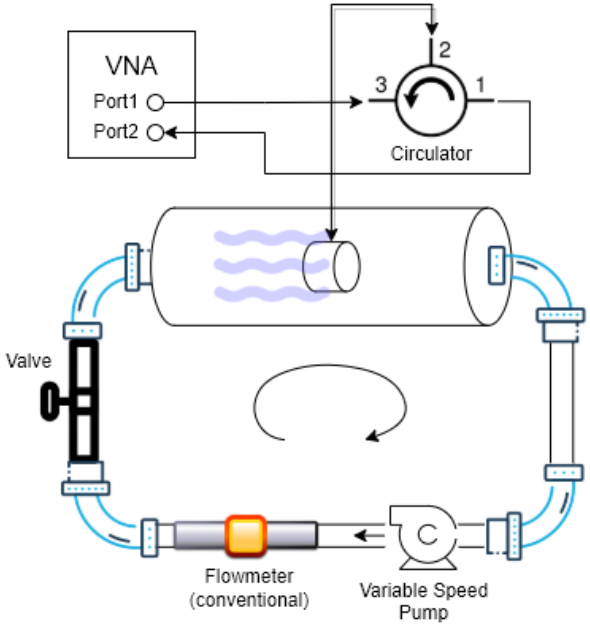

# FLOW SENSING IN WATER LOOP

Obtained initial results of water flow measurement

- Measure frequency shift of $TE_{011}$ mode vs. reference volume flow rate
  - Calculated $f_0$ = 17.80GHz
  - Measured $f_0$ = 17.78GHz
- Sensitivity to flow ≈ 100KHz/GPM

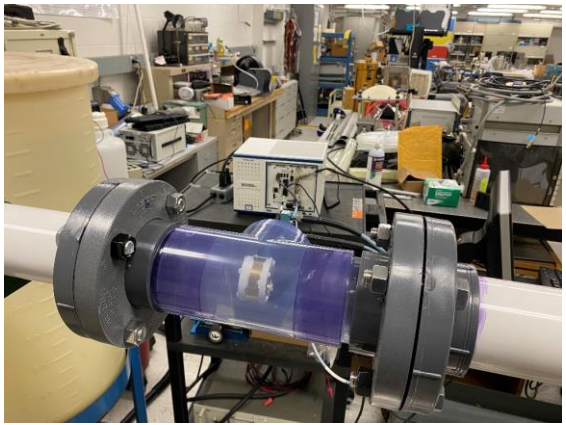

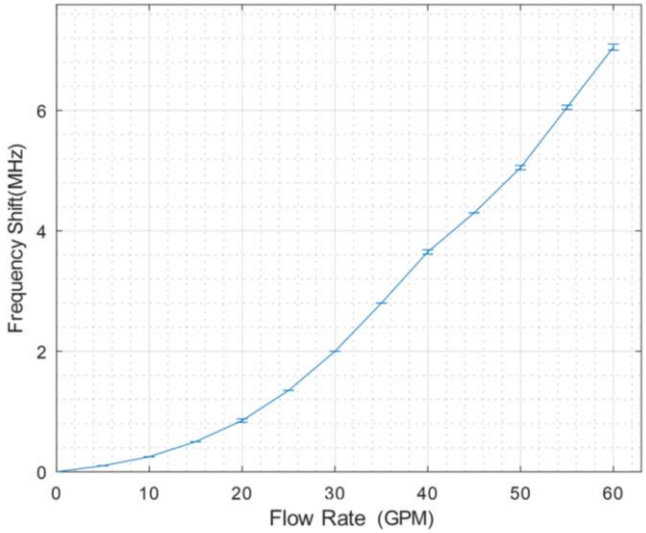


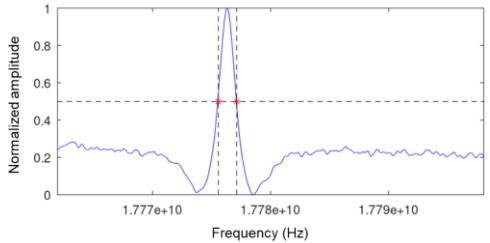


Estimated Q≈11,000

$$Q = \frac{f_0}{\Delta f_{FWHM}}$$

A. Heifetz and S. Bakhtiari, “Microwave Resonant Cavity Transducer for High Temperature Fluid Flow Sensing,” IN-20-146, Argonne National Laboratory (2020).

# TRANSITION TO FLOW SENSING IN LIQUID SODIUM

Identified existing experimental setup for liquid sodium flow sensing test

- Impinging jet flow
- Insulated cylindrical tank 19.5in x 9.5in with ½in center feed line
- Reference ultrasonic flow meter installed on EM pump

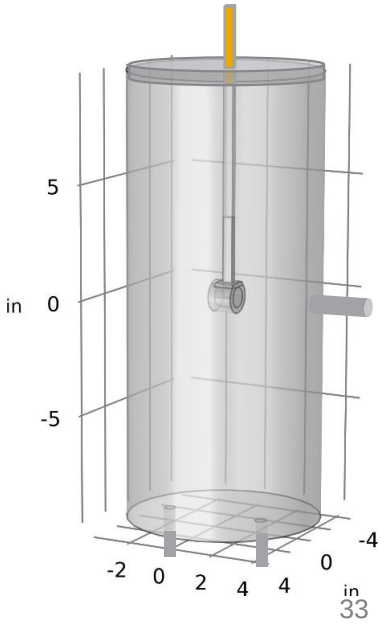


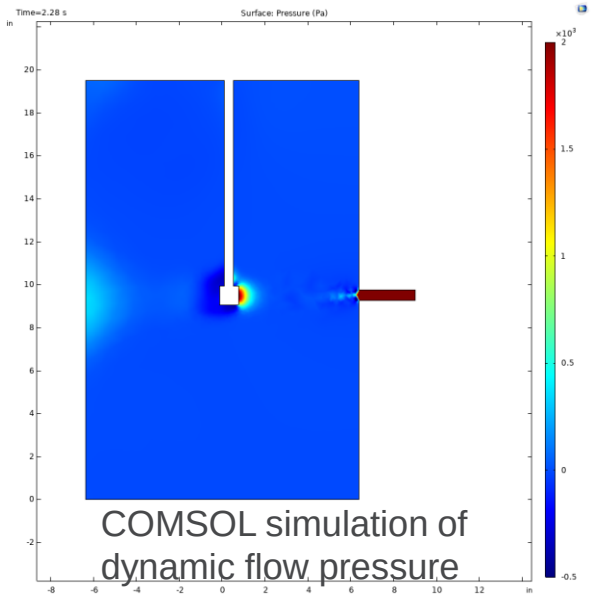


COMSOL simulation of dynamic flow pressure

# TRANSITION TO FLOW SENSING IN LIQUID SODIUM

Developed vessel integrated into loop for flow sensing in impinging jet geometry

- Water vessel with the same geometrical parameters as liquid sodium vessel (20in x 10in cylinder with ½ in center feed line

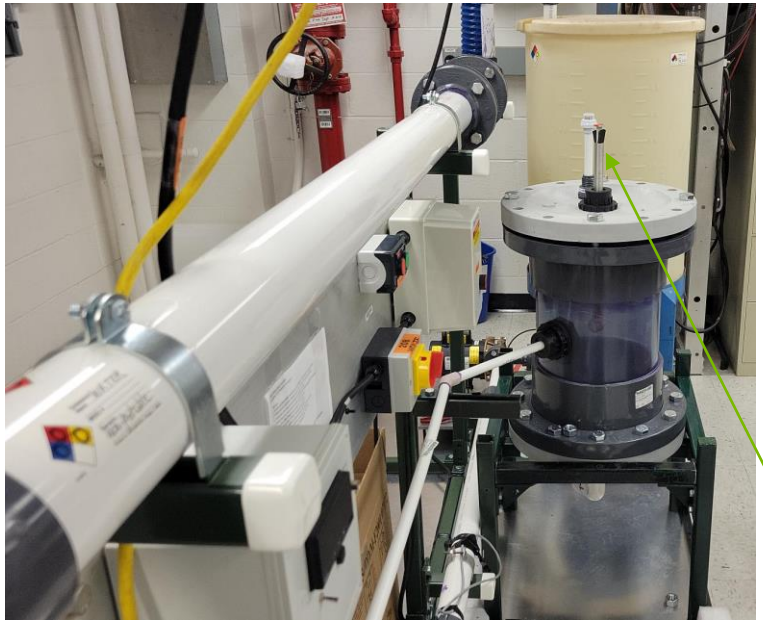

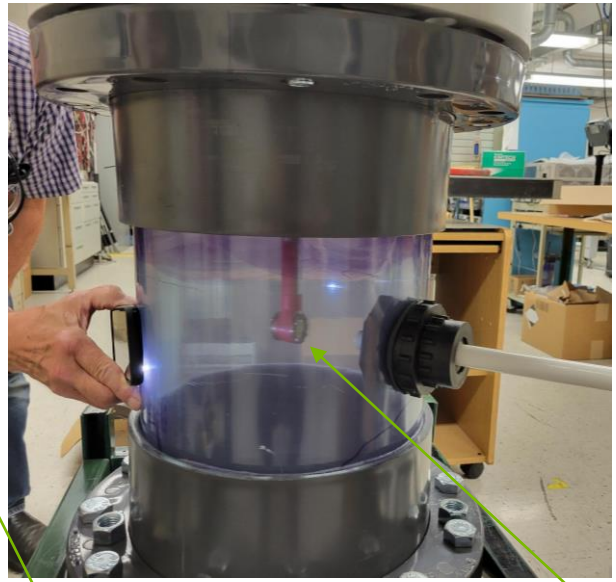

Waveguide insertion probe with cylindrical sensor

# REDESIGNED INSERTION PROBE FOR FLOW SENSING IN WATER VESSEL

- 20in-long K-bad microwave waveguide
- Enclosed in SS316 protective tube

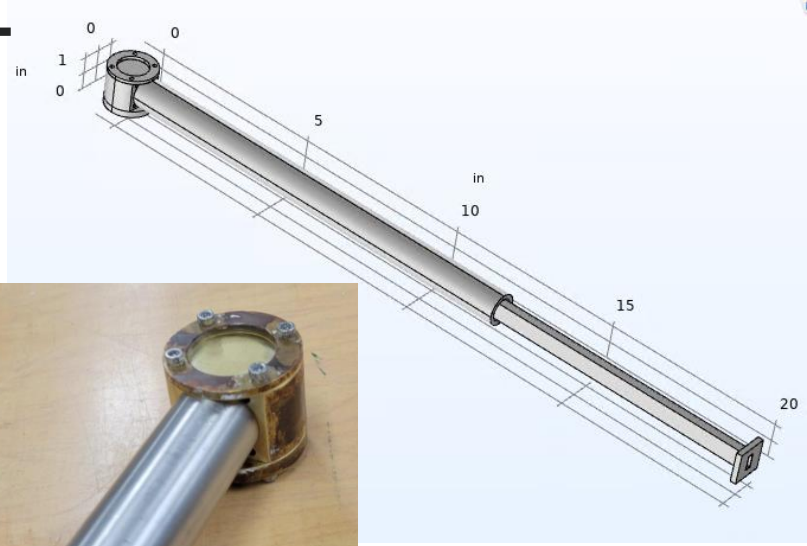


Original K-band rectangular flange

Modified circular-chamfered flange with protective SS316 tube 0.875in diameter and 0.065in wall thickness

# PRELIMINARY RESULTS OF FLOW SENSING IN WATER VESSEL

Preliminary results of flow sensing in water vessel

- Measured frequency shift of $TE_{011}$ mode vs. reference volume water flow rate
  - Calculated $f_0$ = 17.80GHz
  - Measured $f_0$ = 17.78GHz
- Sensitivity to flow ≈ 100KHz/GPM
  - Need to adjust for increasing temperature in fluid

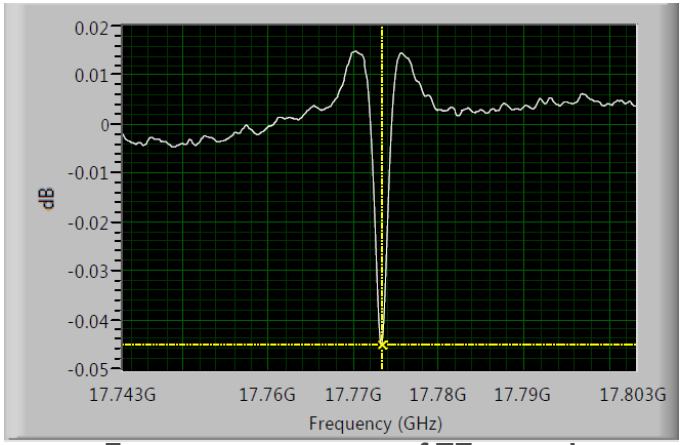


Frequency response of $TE_{011}$ mode

T. Fang, J. Saniie, S. Bakhtiari, A. Heifetz, "Frequency Shift Baseline Removal for Improved Measurement using Microwave Cavity Resonator," Proceedings of *2022 International Conference on Electro-Information Technology* (*EIT*), 436-439.

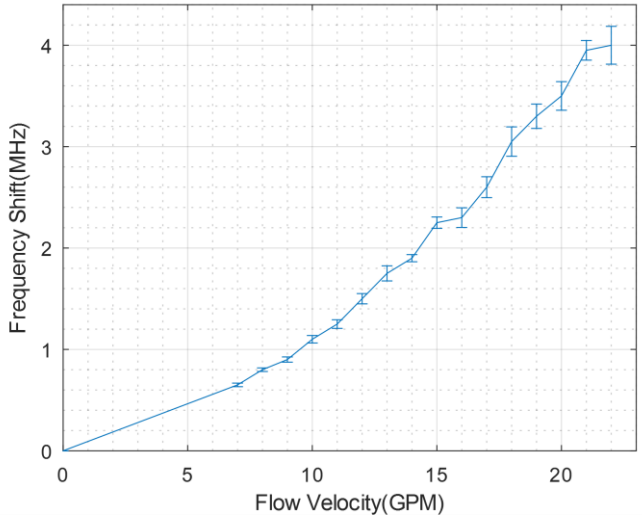

# DESIGNED PROBE ASSEMBLY FOR LIQUID SODIUM FLOW TEST

Designed probe assembly for liquid sodium flow test

- Stainless steel 316 welded structures
- Silver-plated interior surfaces to achieve high Q of resonator

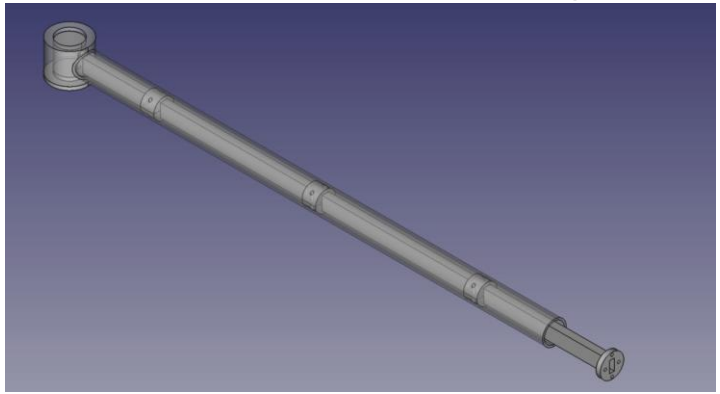

# PRELIMINARY TESTING OF SS316 PROBE IN WATER VESSEL

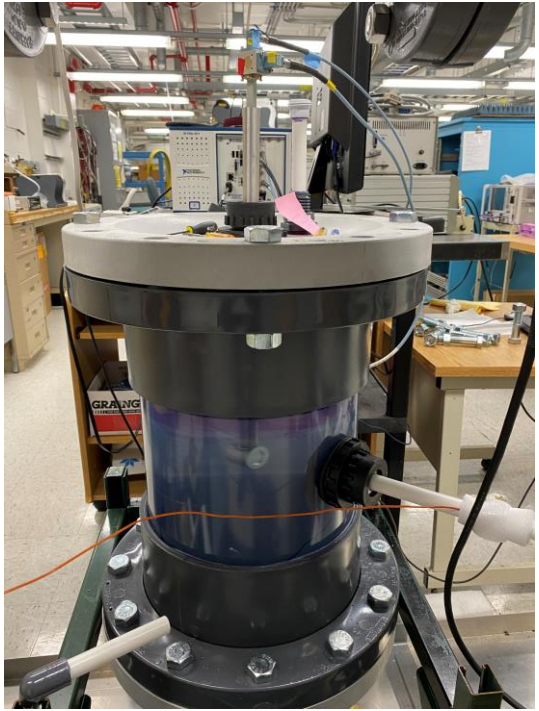

# DESIGNED VESSEL FLANGE FOR PROBE INSERTION

- **Currently under fabrication**

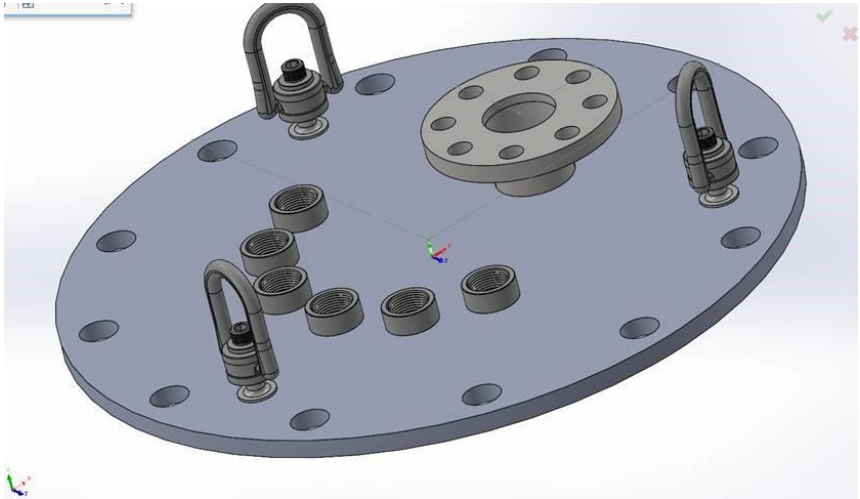

# QUESTIONS?

Alexander Heifetz
Argonne National Laboratory
aheifetz@anl.gov
(630)252-4429